Supplemental material

Hill et al., https://doi.org/10.1084/jem.20190301

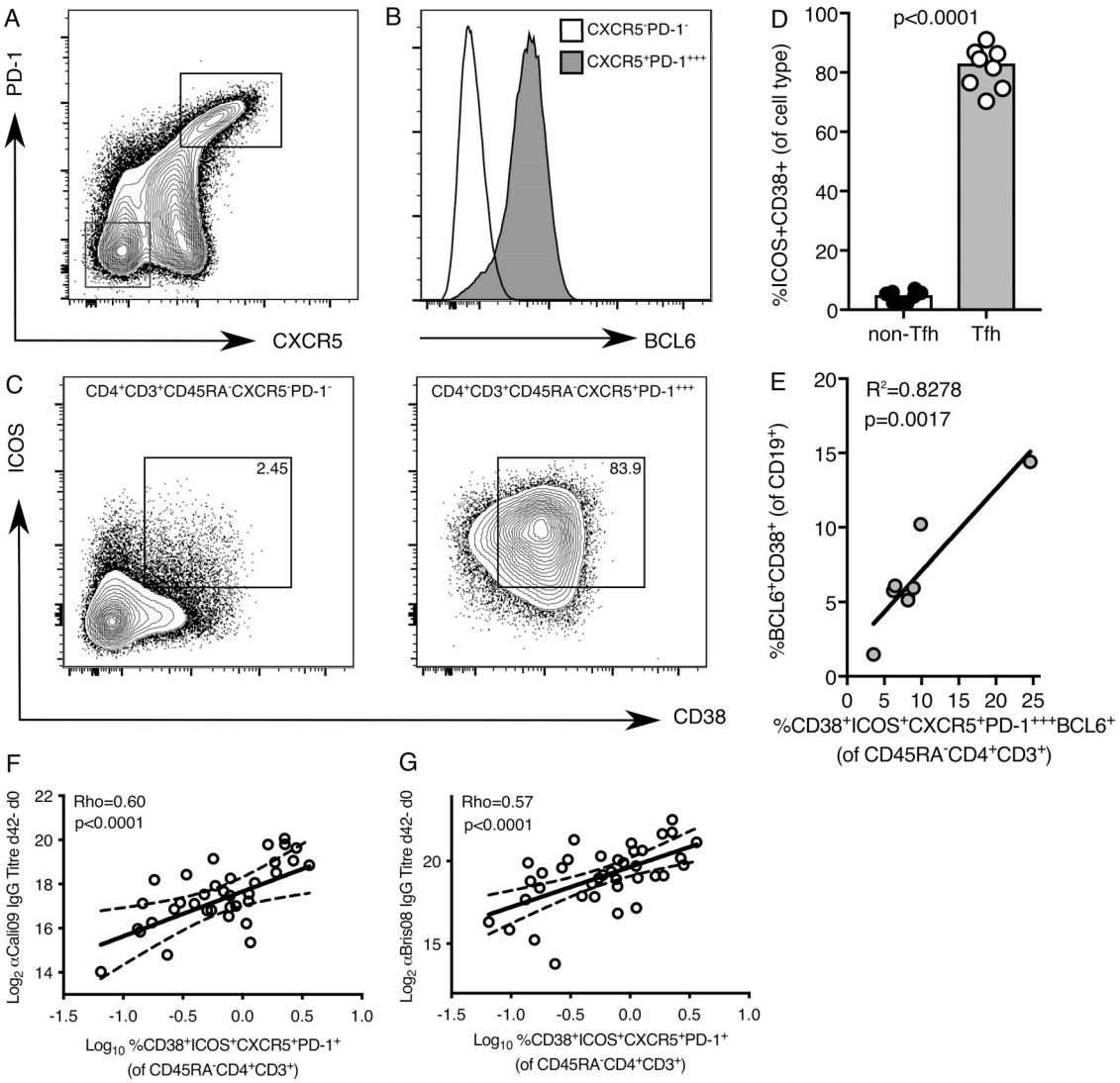

Figure S1. **Tonsil Tfh cells express CD38 and ICOS. (A and B)** Flow cytometric identification of (A) CXCR5⁺PD-1⁺⁺⁺ Tfh cells and CXCR5⁻PD-1⁻ non-Tfh cells among CD45RA⁻CD4⁺CD3⁺ tonsil cells and their expression of BCL6 (B). **(C and D)** Contour plots (C) and quantification (D) of ICOS and CD38 expression on tonsil non-Tfh (left) and Tfh cells (right); n = 8. P < 0.0001. The P value was calculated by a Mann-Whitney test. **(E)** Linear regression analysis of tonsil BCL6⁺CD38⁺CD19⁺ GC B cells and BCL6⁺CD38⁺ICOS⁺CXCR5⁺PD-1⁺⁺⁺ Tfh cells; n = 7. R^2 = 0.8278; P = 0.0017. Each symbol represents one individual. Data are representative of one independent experiment. **(F and G)** Correlation of the frequency of CD38⁺ICOS⁺CXCR5⁺PD-1⁺ cTfh cells 7 d after vaccination with the change in antibody titer of anti-Cal09 IgG (F, an influenza A HA; Rho = 0.60; P < 0.0001) and anti-Bris08 IgG (G, an influenza B HA; Rho = 0.57; P < 0.0001) 42 d after vaccination. Statistical analysis by Spearman's correlation (Rho = coefficient); n = 41. F and G are from one seasonal influenza vaccination cohort.

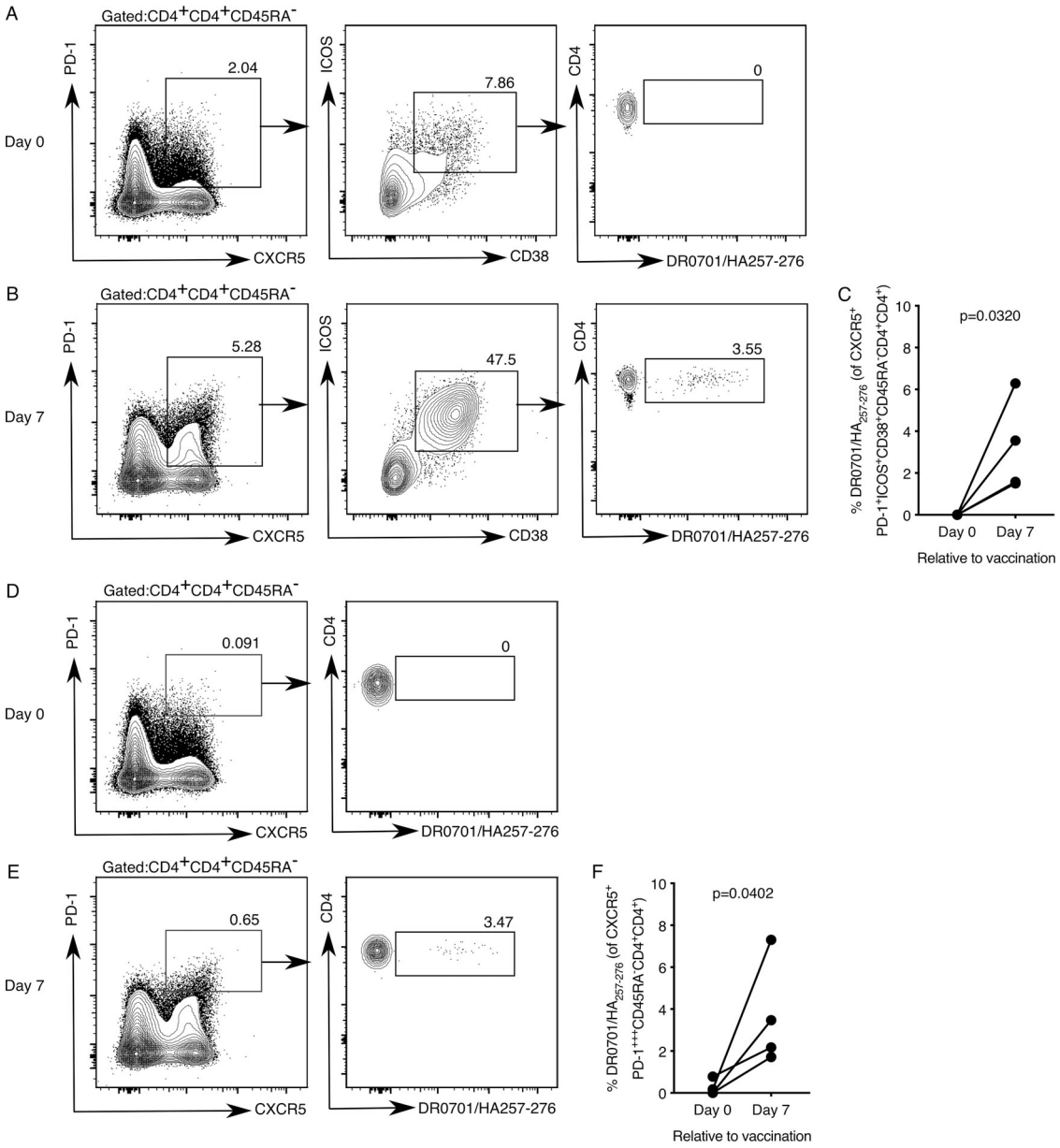

Figure S2. **HA-specific cTfh cells can be identified 7 d after seasonal influenza vaccination. (A–C)** Flow cytometric contour plots (A and B) and quantification (C) of the frequency of HLADR0701/$HA_{257-276}$ tetramer binding cells among $CD38^+ICOS^+CXCR5^+PD\text{-}1^+CD45RA^-CD4^+CD3^+$ cells in the peripheral blood of healthy UK donors at days 0 and 7 relative to seasonal influenza vaccination; $n = 4$. In C, each symbol represents a volunteer; an individual donor is connected by a line at the two time points; $n = 4$. P = 0.0320. The P value was generated with a paired Student's *t* test. **(D–F)** Flow cytometric contour plots (D and E) and quantification (F) of the frequency of HLADR0701/$HA_{257-276}$ tetramer binding cells among $CXCR5^+PD\text{-}1^{+++}CD45RA^-CD4^+CD3^+$ cells in the peripheral blood of healthy UK donors at days 0 and 7 relative to seasonal influenza vaccination; $n = 4$. In F, each symbol represents a volunteer; an individual donor is connected by a line at the two time points; $n = 4$. P = 0.0402. The P value was generated with a paired Student's *t* test. Data are from one seasonal influenza cohort.

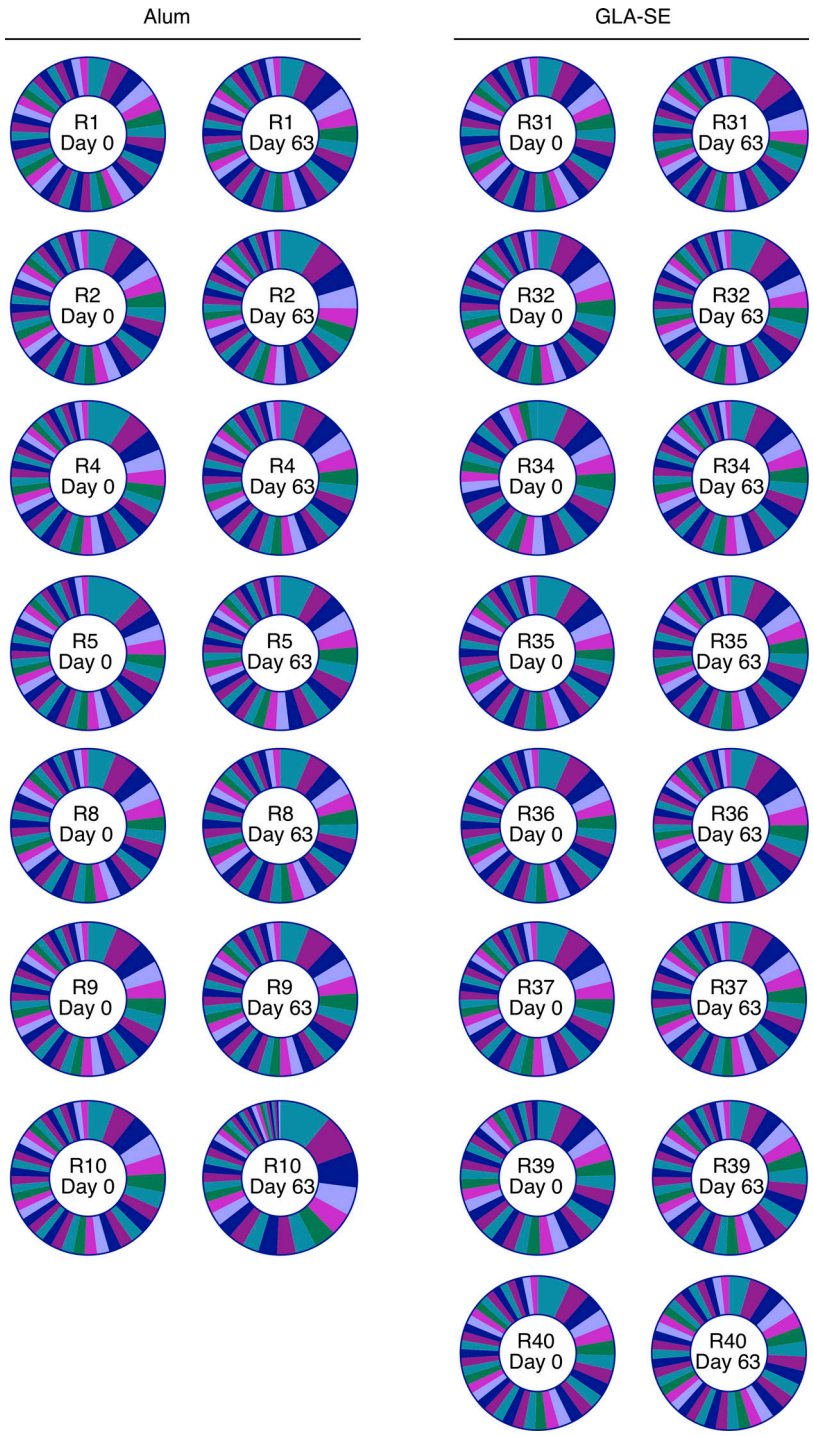

Figure S3. **Abundance of TCRβ CDR3 clonotypes in cTfh cells.** Pie charts of the proportion of the 40 most abundant TCRβ CDR3 clonotypes in ICOS$^+$CD38$^+$CXCR5$^+$PD-1$^+$ cTfh cells of individual P27A study participants at the indicated study time points. Alum group, n = 7; GLA-SE group, n = 8. Each segment of the pie chart represents a unique CDR3 clonotype. The "R" number is the unique participant identifier. Data are from one clinical trial.

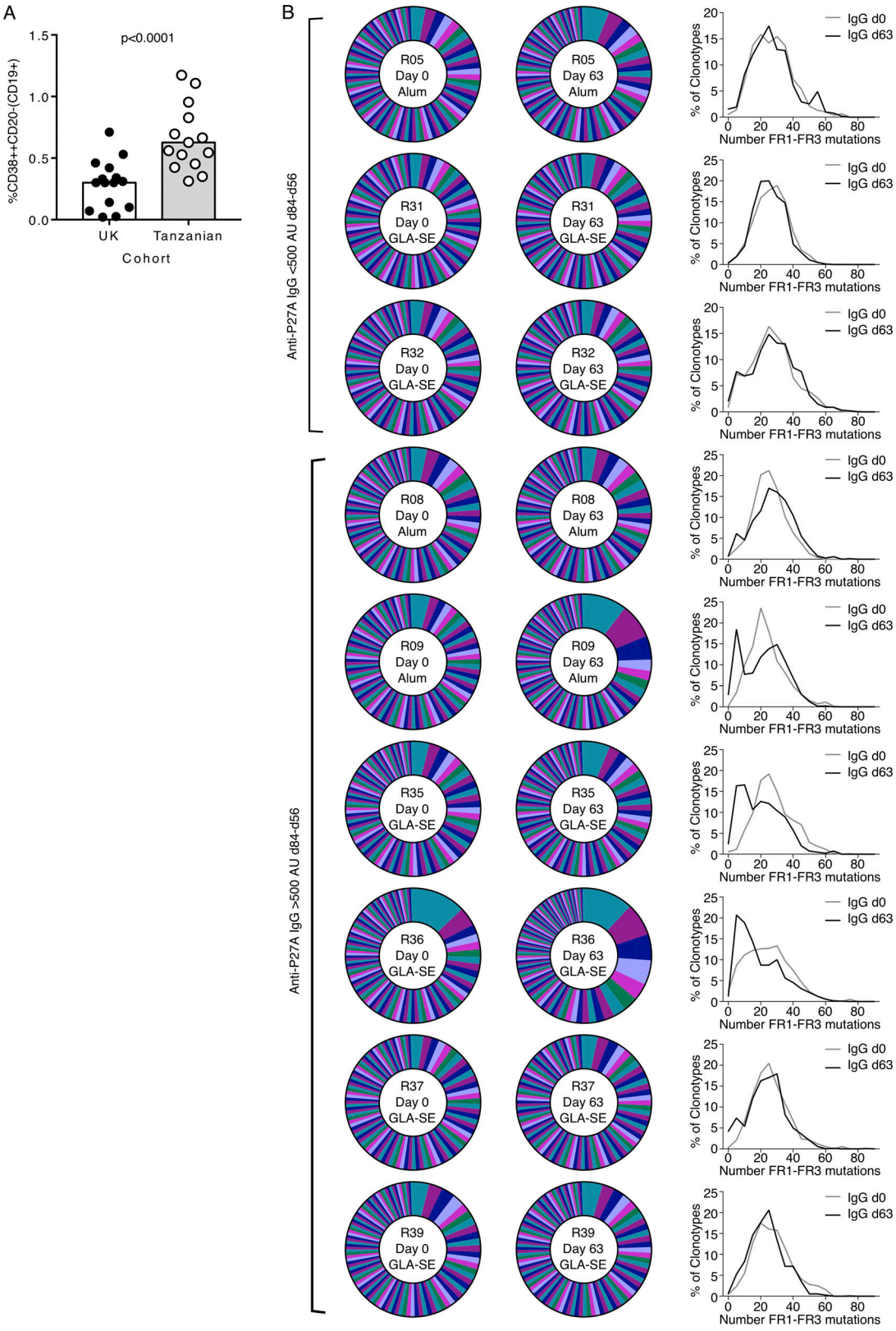

Figure S4. **Tanzanian volunteers had a higher ASC frequency before vaccination and V(D)J sequencing of circulating plasmablasts. (A)** Percentage of $CD19^+$ lymphocytes that are $CD38^{2+}CD20^-$ in 18–45-yr-olds from either the UK (n = 15) or Tanzania (n = 15) before vaccination. P < 0.0001. The P value was calculated from a Mann-Whitney U test. **(B)** Pie charts of the proportion of the 100 most abundant BCR clonotypes in $CD38^{2+}CD20^-CD19^+$ ASCs of individual P27A study participants at the indicated study time points. Each segment of the pie chart represents a unique BCR clonotype (FR1–FR4 regions). Alum group, n = 3; GLA-SE group, n = 6. The "R" number is the unique participant identifier. Line graphs show the number of mutations in the V region per clonotype (FR1–FR3, split into bins of five mutations) in each individual before vaccination and 7 d after the third vaccination (d63). Data are from one clinical trial.

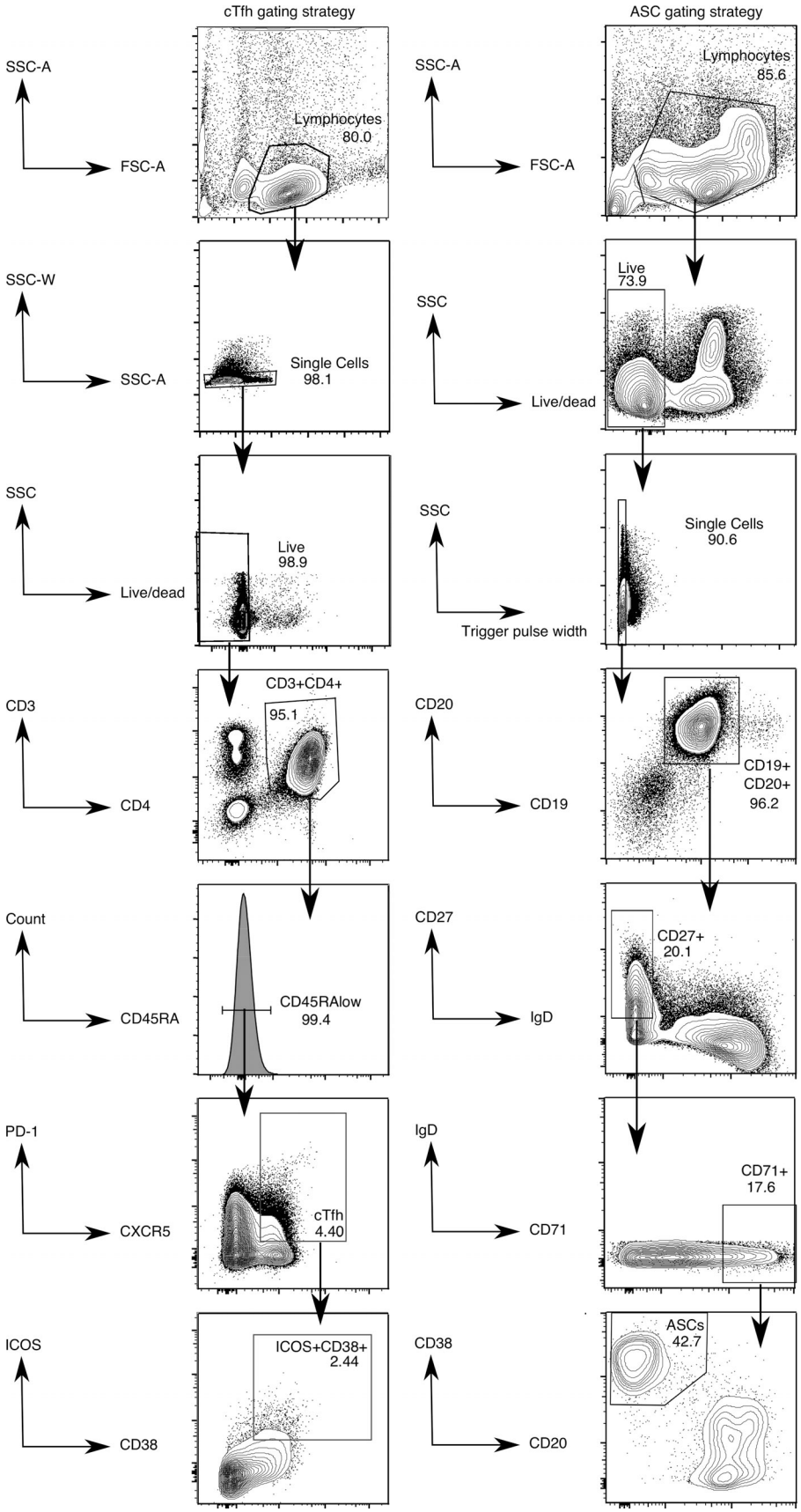

Figure S5. **Gating strategy for fluorescence-activated cell sorting of cTfh and ASCs.** Representative flow cytometry plots for the gating strategy for cTfh cells (left) and ASCs (right) with parameter axes labels shown alongside.